

Article

Investigation and Optimization of Co-Combustion Efficiency of Food Waste Biochar and Coal

Yoonah Jeong ^{1,†}, Jae-Sung Kim ^{2,†}, Ye-Eun Lee ¹ , Dong-Chul Shin ^{1,3} , Kwang-Ho Ahn ¹ , Jinhong Jung ¹, Kyeong-Ho Kim ² , Min-Jong Ku ², Seung-Mo Kim ⁴, Chung-Hwan Jeon ^{2,4,*}  and I-Tae Kim ^{1,*} 

¹ Department of Environmental Research, Korea Institute of Civil Engineering and Building Technology, Goyang-daero 283, Ilsanseo-gu, Goyang-si 10223, Republic of Korea; yoonahjeong@kict.re.kr (Y.J.); yeeunlee@kict.re.kr (Y.-E.L.); dcshin@daejin.ac.kr (D.-C.S.); khahn@kict.re.kr (K.-H.A.); jinhong98@kict.re.kr (J.J.)

² School of Mechanical Engineering, Pusan National University, 2, Busandaehak-ro 63 beon-gil, Geumjeong-gu, Busan 46241, Republic of Korea; e1223kjs@pusan.ac.kr (J.-S.K.); kkh751@pusan.ac.kr (K.-H.K.); tbvjalswhd@pusan.ac.kr (M.-J.K.)

³ Department of Smart Construction and Environmental Engineering, Daejin University, 1007 Hoguk-ro, Pocheon-si 11159, Republic of Korea

⁴ Pusan Clean Energy Research Institute, Pusan National University, 2, Busandaehak-ro 63 beon-gil, Geumjeong-gu, Busan 46241, Republic of Korea; kims@pusan.ac.kr

* Correspondence: chjeon@pusan.ac.kr (C.-H.J.); itkim@kict.re.kr (I.-T.K.)

† These authors contributed equally to this work.

Abstract: Among the alternative recycling methods for food waste, its utilization as a renewable biomass resource has demonstrated great potential. This study presents empirical findings pertaining to the cofiring of solid biomass fuel and coal for power generation. Various co-combustion ratios involving food waste biochar (FWB) and coal (100:0, 85:15, 90:10, 95:5, and 0:100) were tested to optimize combustion efficiency, monitor the emissions of NO_x, CO, and unburned carbon (UBC), assess ash deposition tendencies, and evaluate grindability. Two types of FWB and sewage sludge were selected as biomass fuels. The results demonstrated that co-combustion involving FWB reduced NO_x and UBC emissions compared to coal combustion alone. In particular, the 10% FWB_A blend exhibited the best combustion efficiency. Notably, FWB demonstrated lower tendencies for ash deposition. The ash fusion characteristics were monitored via thermomechanical analysis (TMA), and the corresponding shrinkage levels were measured. Furthermore, FWB exhibited superior grindability compared to both coal and sewage sludge, reducing power consumption during fuel preparation. This study suggests that FWB is a valuable co-combustion resource in coal-fired power plants, thereby facilitating the efficient recycling of food waste while concurrently advancing clean energy generation. Nevertheless, further research is required to validate its practical applicability and promote its use as a renewable resource.

Keywords: biomass; food waste biochar; co-combustion (co-pyrolysis); thermomechanical analysis; drop tube furnace; slagging; fouling; grindability



Citation: Jeong, Y.; Kim, J.-S.; Lee, Y.-E.; Shin, D.-C.; Ahn, K.-H.; Jung, J.; Kim, K.-H.; Ku, M.-J.; Kim, S.-M.; Jeon, C.-H.; et al. Investigation and Optimization of Co-Combustion Efficiency of Food Waste Biochar and Coal. *Sustainability* **2023**, *15*, 14596. <https://doi.org/10.3390/su151914596>

Academic Editors: Steven Lim, Shuit Siew Hoong, Santi Chuetor and Pang Yean Ling

Received: 7 September 2023

Revised: 2 October 2023

Accepted: 6 October 2023

Published: 8 October 2023



Copyright: © 2023 by the authors. Licensee MDPI, Basel, Switzerland. This article is an open access article distributed under the terms and conditions of the Creative Commons Attribution (CC BY) license (<https://creativecommons.org/licenses/by/4.0/>).

1. Introduction

The combustion of biomass fuels for power generation has garnered considerable attention because of the carbon-neutral nature of biomass. The benefits of cofiring biomass, including reduced greenhouse gas emissions, low cost, broad availability, and simple application in plant facilities, have promoted its implementation in power generation [1,2]. Although various types of biomass fuels, such as sewage sludge, have been employed [3,4], this study focused on food waste as a renewable biomass resource. The recycling rate of food waste reached 96% in the Republic of Korea in 2019 [5]. However, because of limitations in the recycling approaches, including feedstock, fertilization, and bio-gasification, the development of alternative recycling methods targeting food waste is urgently needed. As

an alternative recycling method, food waste is converted into food waste biochar (FWB) via pyrolysis and demineralization. FWB, a solid product of pyrolyzed biomass, has shown potential as a fuel owing to its high calorific value, high recycling rate in Korea, and low chlorine and heavy metal contents [6,7].

The combustion of biomass may cause several issues in facility operations because of the various combustion behaviors of different fuels and difficulties in their preparation. In particular, ash fusion characteristics during the cofiring of biomass and coal have been reported [8]. High inorganic contents such as alkali and alkali earth metals in biomass ash lead to slagging, fouling, and corrosion [9–11]. The operating temperature of a biomass-fired boiler decreases because of the attached biomass ash on its surface. Such inorganic ash compositions in biomass eventually lower the combustion efficiency and cause maintenance issues. Accordingly, when biomass and coal are cofired, ash fusion tests of the biomass by thermomechanical analysis (TMA) must be conducted to predict key technical problems, such as slagging tendencies [12,13]. For example, the shrinkage of biomass fuels with increasing temperatures can be examined using TMA.

Another undesirable characteristic of biomass is its poor grindability [14,15]. A grinding procedure is required for the preparation of fuel to maintain the homogeneous size of both the biomass and coal before combustion. Fuel particle size is a key factor in efficient combustion. In general, grindability is a critical problem in biomass cofiring because of the high grindability index resulting from the fibrous nature of the biomass. Biomass with poor grindability undergoes an additional fragmentation process, which requires more time and cost.

This study set out to assess the feasibility of cofiring FWB and coal. To substantiate the sustainability and environmental friendliness of cofiring FWB, this study investigates the co-combustion of FWB and coal while monitoring the combustibility, ash deposition characteristics, ash fusion tendencies, and FWB grindability. Various mixing ratios between the FWB and coal were tested to determine the optimal operating conditions and maximize combustion efficiency. Considering that most biomass is cofired at approximately 3–5%, mixing ratios of 0%, 5%, 10%, 15%, and 100% FWB were used in this study. Sewage sludge, another biomass fuel that is currently used in coal-fired power plants, was selected to compare its overall co-combustion characteristics with those of FWB. A drop tube furnace (DTF) was used to investigate NO_x, CO, CO₂, and unburned carbon (UBC) emissions from cofiring. The ash deposition and fusion characteristics were also experimentally studied. Because ash fusion characteristics are difficult to estimate from a single TMA, TMA was conducted for all mixing ratios to observe changes in ash fusion trends with increasing cofiring FWB ratio. To the best of our knowledge, this represents the first endeavor to undertake an exhaustive analysis of the cofiring of FWB and to optimize co-combustion ratios between FWB and coal. The authors believe that the results of this study will encourage the use of FWB as a cofiring biomass fuel in coal-fired power plants.

2. Materials and Methods

2.1. Preparation of Solid Fuel

This study used two types of FWBs and sewage sludge as biomass. Food waste was converted into FWB_A and FWB_B via pyrolysis and demineralization. The food waste procured from the Gimpo Urban Management Corporation (Gimpo-si, Republic of Korea) was shredded and dehydrated. FWB_A was produced through the pyrolysis of dried food waste at 500 °C for 20 min. Pyrolyzed FWB was then demineralized using acidified water (i.e., 3% citric acid) to reduce the chlorine content of the FWB, which was referred to as FWB_A. This demineralization step was imperative due to the potential emission of dioxin and dioxin-like substances associated with the high chlorine content in FWB [16]. The detailed preparation process has been described in a previous study [17]. FWB_B was produced following the same protocol, albeit employing a slightly different demineralization method involving deionized water. Before the experiment, FWB_A and

FWB_B were sieved through a 2 mm mesh. Subsequent to the preparation procedures, the yield of FWB ranged between 43.2% and 53.8%.

The sludge and coal were provided by Korea Midland Power. The preparation of all samples involved an initial milling process followed by sieving to achieve a particle size distribution within the range of 75 μm to 125 μm . A sieve shaker (AS 200, Retsch GmbH, Haan, Germany) was employed for this purpose. Subsequent to the size reduction, the samples were subjected to air drying based on the air-dried moisture content. The experimental settings used in this study for biomass and coal are listed in Table 1.

Table 1. Experimental ratios of the coal and biomass fuels.

	Combustion			Co-Combustion			
Coal	100%	0%	95%	90%	85%	85%	85%
FWB_A	0%	100%	5%	10%	15%	0%	0%
FWB_B	0%	0%	0%	0%	0%	15%	0%
Sewage sludge	0%	0%	0%	0%	0%	0%	15%

FWB: food waste biochar.

2.2. Characterization of Biomass and Coal

The fuel properties of biomass and coal were investigated via proximate analyses, heating values, and elemental analyses. A thermogravimetric analyzer (TGA 701, LECO Co., St. Joseph, MI, USA) was used for the proximate analysis based on the American Society for Testing and Materials (ASTM) guidelines: ASTM D3173-11 for analytical moisture, ASTM D3175-11 for volatile matter, ASTM D3174-12 for ash, and ASTM D3172-13 for fixed carbon [18–21]. The net calorific value was measured using a bomb calorimeter (5E-C5508, CKIC, Changsha, China) according to ASTM D5865 [22]. The ash composition was determined using X-ray Fluorescence (XRF) following the German standard (DIN 51729-10) [23].

2.3. Combustion Test Using DTF

In this experiment, a DTF was used to investigate the combustion emission characteristics of NO_x , CO, CO_2 , and UBC. A DTF has the advantage of maintaining a uniform temperature and allowing for experiments over a wide range of temperatures. A schematic representation of the experimental apparatus used in this study is shown in Figure 1 [24]. The experimental unit consists of a feeding section for injecting a mixture of pulverized coal and biomass, a reaction section where the combustion reaction occurs, and a collection section for capturing the combustion gases. The feeding part consists of injecting fuel and reaction gas, which are divided into carrier gas and primary reaction gas streams. The flow rate of the main reaction gas, which was directly injected into the reactor, was controlled using a mass flow controller. The fuel and reactive gases meet, and chemical reactions occur in the reaction section. A SiC heater is used to maintain a constant temperature, which can reach up to 1500 $^\circ\text{C}$.

To minimize experimental errors, each experimental condition underwent three iterations. A real-time gas analyzer was used to measure the composition of the exhaust gas at the rear of the DTF once per second. UBC was measured using the ash tracer method [25]. This approach was necessitated by the limited amount of char or ash available for direct comparison with the amount of fuel. The method operates on the assumption of constancy in the ash content of the fuel before and after combustion to determine the UBC of the fuel by comparing its ash content before and after combustion using a proportional formula. The formula used is as follows:

$$\text{UBC (\%)} = \left[1 - \frac{A_0(100 - A_{char})}{A_{char}(100 - A_0)} \right] \times 100 \quad (1)$$

where A_0 is the ash content of the raw coal and A_{char} is the ash content of the char captured after the reaction.

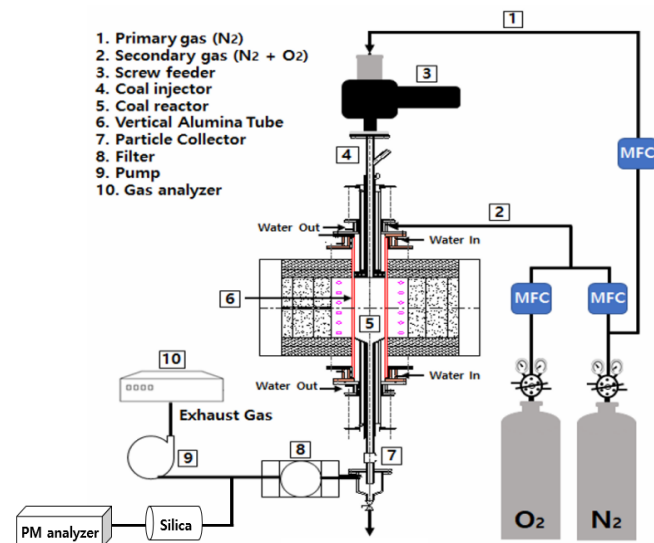


Figure 1. Schematic representation of the experimental drop tube furnace setup.

2.4. Ash Deposition Test Using DTF

An ash deposition experiment was performed using a probe placed at the bottom of the DTF. Ten grams of biomass were supplied at a feeding rate of 0.2 g/min at 1300 °C. Ash deposition was measured using capture efficiency (CE) and energy-based growth rate (GRE) as indicators [26,27]. The CE was obtained by dividing the deposited mass by the mass of ash particles flowing along the surface area of the probe during the experiment (Equation (2)).

$$CE = \frac{m_{Dep}}{m_{Fuel} \left(\frac{A^P}{100} \right) \left(\frac{A_{coupon}}{A_{reactor}} \right)} \times 100 \text{ [%kg}_{Dep}/\text{kg}_{Ash}] \quad (2)$$

where m_{Dep} and m_{Fuel} represent the mass (kg) of ash deposited on the coupon surface and fuel supplied during the experiment, respectively. A^P , A_{coupon} , and $A_{reactor}$ are the ash content (wet basis) in the fuel, the projected area of the coupon, and the cross-sectional area of the DTF, respectively, where A denotes the amount of ash in the fuel. While the CE helps in understanding the tendency of the adherent ash fraction, it may inadvertently neglect the influence of the mineral components within the solid fuel and the correlation between the solid fuel and its calorific value. To surmount this limitation, the GRE was calculated as follows (Equation (3)):

$$GRE = \frac{m_{Dep}}{LHV \cdot m_{Fuel}} \text{ [%g}_{Dep}/\text{MJ}] \quad (3)$$

The GRE is an indicator of the amount of ash deposition relative to the total energy supplied to the solid fuel (mass unit: g). LHV represents the low heating value (MJ). The characteristics of ash from solid fuels and the ash deposition rate based on energy can be estimated using GRE.

2.5. Ash Fusion Behavior Test Using TMA

Melting experiments were conducted using TMA to analyze the melting tendencies of ash particles in biomass fuel [28]. TMA was designed and fabricated at the Pusan Clean Energy Institute at Pusan National University. The measurement method involved placing a graphite crucible containing the sample on an alumina holder and positioning an alumina rod on top of the sample. The crucible was then heated under a nitrogen atmosphere up to 1600 °C, whereas the shrinkage rate of the sample was measured using a displacement gauge. The shrinkage rate refers to the value obtained by dividing the shrinkage at each temperature by the total shrinkage displacement. The experimental results are denoted as TX%, where X% signifies the temperature at which the shrinkage rate reaches X%. The schematic diagram of the TMA apparatus is presented in Figure 2.

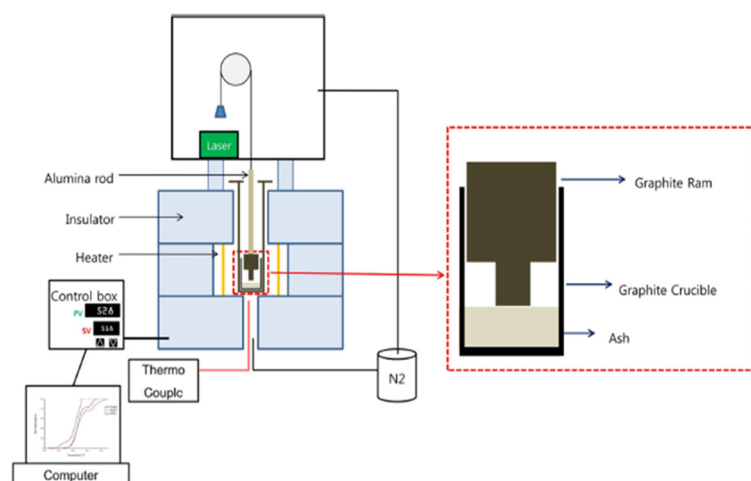


Figure 2. Schematic representation of TMA.

2.6. Evaluation of Grindability

The grindability of the solid fuel was measured using the Hardgrove Grindability Index (HGI), following the guidelines outlined in the Japanese Industrial Standard M8801 [28]. Over 300 g of the solid fuel underwent grinding within the particle size range of 0.6 mm to 1.18 mm. Pulverized solid fuels (50 g) were placed in a grinding bowl under a pressure of 284 N. The grinding bowl was operated at both 20 rpm and 60 rpm. Solid fuels sieved through a 75 μm sieve were recorded to calculate the HGI, which was further modified into the Thermally Treated Biomass Grindability Index (TTBGI) [29,30]. In this study, the grindability of biomass samples was measured via the TTBGI method and leveraging HGI (5E-HA60 \times 50, Changsha Kaiyuan Instruments Co., Changsha, China) equipment.

3. Results and Discussion

3.1. Characterization of Biomass and Coal

The proximate and ultimate analyses of the solid fuels are presented in Table 2. FWB_A exhibited the highest fixed carbon content, with a subsequent decrease observed in the following order: coal > FWB_B > sewage sludge. The low fixed carbon content in sewage sludge can be attributed, in part, to its predominant volatile matter, which surpasses that of other solid fuels by approximately twofold. From the ultimate analysis, it becomes evident that FWB_A, FWB_B, and the sludge contain notably elevated N levels (>7%) compared with coal. Furthermore, both FWB variants displayed lower sulfur (S) contents than those of coal and sewage sludge. Intriguingly, FWB_A and coal exhibited similar calorific values, whereas the lowest calorific value observed in the sludge can be attributed to its high oxygen and low carbon contents.

Table 2. Proximate and ultimate analyses of solid fuels.

	Coal	FWB_A	FWB_B	Sewage Sludge
Proximate analysis				
Moisture (%)	2.24	3.49	3.56	5.07
Volatile matter (%)	25.59	30.92	30.93	61.05
Fixed C (%)	51.90	54.84	46.45	9.58
Ash (%)	20.26	10.75	19.07	24.30
Ultimate analysis				
C (%)	78.73	73.43	69.97	48.18
H (%)	5.16	4.35	4.22	7.21
N (%)	4.26	7.27	7.28	7.83
S (%)	0.27	0.04	0.11	0.84
O (%)	11.57	14.91	18.41	35.93
Net calorific value (kcal/kg)	6244	6167	5286	4084

3.2. Gaseous Emissions from the Combustion of Solid Fuels

The gaseous emissions, including NO_x , CO, CO_2 , and UBC, from the combustion of solid fuels are shown in Figure 3. As depicted in the figure, all co-combustion cases involving FWB_A and FWB_B exhibited reduced NO_x emissions compared to the combustion of coal or FWB_A alone. The NO_x concentrations ranged from 96.38 ppm (5% FWB_A) to 136.08 ppm (100% coal). Generally, the incorporation of biomass in cofiring significantly mitigated both NO_x and SO_x emissions [31,32]. The combustion of 100% FWB_A yielded the highest NO_x emission, likely attributed to the good combustibility of FWB_A due to its elevated N content and low UBC value. The NO_x emission exhibited a linear increase with increasing FWB_A cofiring ratio. Given the consistency in furnace configuration throughout the testing, discrepancies in NO_x levels likely arise from differences in volatile matter and fuel N contents.

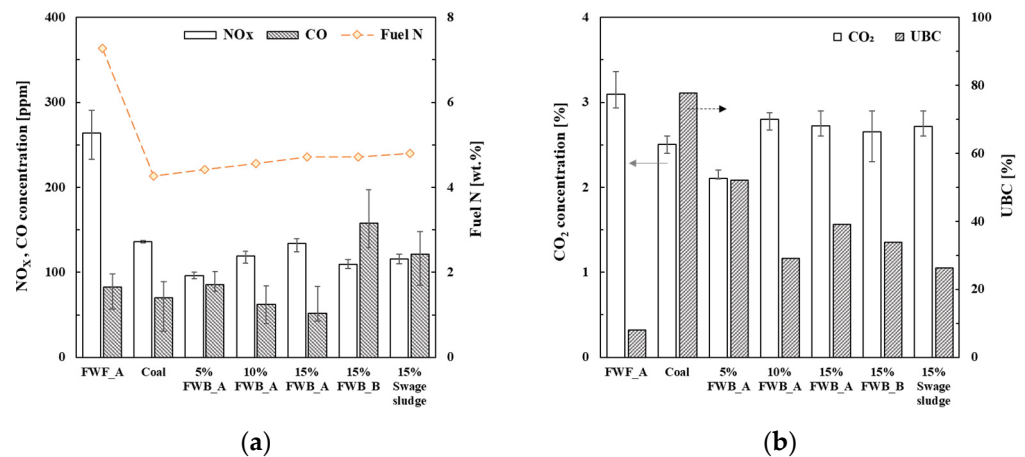


Figure 3. (a) Concentrations of NO_x (blank bar), CO (gray bar), and fuel N (yellow dot line). (b) CO_2 concentrations (blank bar) and unburned carbon (UBC) (gray bar).

CO emissions can be used as an indicator of combustion efficiency [33,34]. Although CO emission levels depend on various factors, such as fuel heterogeneity, size, and distribution, homogeneous fuel generally leads to improved combustion efficiency [35]. For FWB_A, an increased mixing rate corresponded to a reduction in CO concentration. Specifically, CO concentrations for 5% FWB_A, 10% FWB_A, and 15% FWB_A were recorded as 85.23, 62.67, and 51.47 ppm, respectively. Notably, when juxtaposed with the combustion of coal or FWB_A alone, cofiring ratios of 10% FWB_A and 15% FWB_A demonstrated improved combustion efficiencies, as evidenced by their CO concentrations of 70.19 ppm and 83.06 ppm, respectively. Interestingly, the co-combustion of 15% FWB_B and 15% sludge exhibited the highest CO emissions, underscoring the superior combustion efficiency of FWB_A compared to FWB_B and sludge.

The CO_2 emissions (2.10% to 3.09%) remained consistent across all solid fuels. The UBC levels were calculated by measuring the carbon content within the ash after combustion (Equation (1)). In particular, the UBC concentration for 10% FWB_A was lower than that of the other co-combustion ratios. Elevated UBC and CO emissions constitute the primary factors contributing to reduced combustion efficiency [36]. Consequently, the gaseous emission trends suggest that co-combustion with 10% FWB_A was the most effective in achieving minimal NO_x , CO, and UBC emissions.

3.3. Ash Deposition Rate

Reactor fouling and corrosion represent typical challenges inherent to biomass combustion [11,36,37]. Ash deposited on the surface of the reactor functions as an insulating layer, which reduces the heat transfer efficiency. Accordingly, a high ash deposition rate may result in heightened fuel consumption and a reduction in thermal efficiency. Furthermore, excessive ash deposition affects the operation and maintenance of combustion

systems. The accumulated ash may cause flame instability and disturb the flow of gases and the combustion process, necessitating more frequent maintenance intervals to uphold the combustion system's dependable operation. Therefore, a DTF deposition experiment was performed to compare the ash deposition for each biomass sample. Figure 4 shows the deposition characteristics of each biomass sample after combustion, obtained from the results of the DTF deposition experiment.

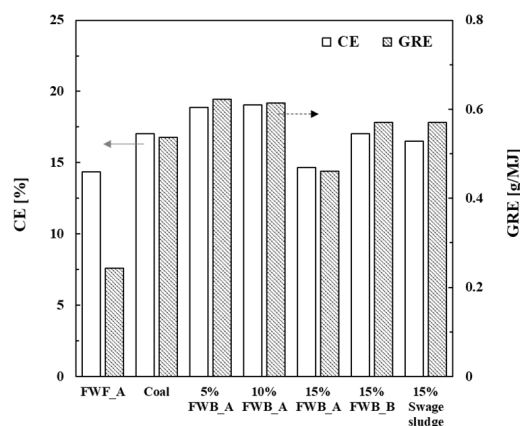


Figure 4. Comparison of capture efficiency (CE, blank bar) and energy-based growth rate (GRE, gray bar) for biomass fuels and coal.

In the context of combustion of coal alone, the CE for coal approached approximately 17%, whereas the CE for 100% FWB_A was 14%. It is noteworthy that the FWBs exhibited relatively lower ash deposition tendencies, as assessed through both the GRE and CE indices. The CE and GRE values for FWB, as determined in this study, are comparably lower than those reported for other biomass [17]. Low ash deposition on the surface of the reactor indicates enhanced heat transfer and thermal efficiency in the combustion process. Additionally, the operational challenges arising from ash deposition constitute a noteworthy consideration in cofiring practices. The co-combustion of biomass and coal can give rise to excessive ash deposition, necessitating heightened maintenance procedures and downtime during combustion. In this regard, FWB presents advantages over other wood and herbaceous biomass.

In the case of co-combustion scenarios involving 15% FWB_A, 15% FWB_B, and 15% sewage sludge, ash CE values were 14.64%, 17.03%, and 16.50%, respectively. Additionally, the ash deposition profiles for 5% FWB_A and 10% FWB_A exhibited similar CE values of 18.86% and 19.05%, respectively. Previous studies have shown that biomass combustion usually yields higher ash deposition rates than those yielded via coal combustion [13]. Our findings in this study align with this pattern, showcasing elevated CE and GRE values for biomass combustion. The smallest accumulated ash mass was observed in the case of FWB_A (100%, 0.062 g). When evaluated in terms of CE and GRE indices, FWB_A at 15% and 100% displayed reduced ash deposition tendencies. It is essential to underline the substantial disparity between GRE and CE in FWB_A combustion, potentially attributable to the distinct definitions of GRE and CE. CE was derived solely from the accumulated ash content without considering the calorific value of the solid fuel, whereas GRE was defined as the deposited ash per calorific value. For instance, complete coal combustion resulted in approximately 0.54 g/MJ, whereas FWB_A yielded 0.24 g/MJ. Co-combustion of 15% FWB_A and coal generated 0.46 g/MJ, while 15% FWB_B and sludge produced 0.57 g/MJ (Figure 4). Furthermore, ash depositions were recorded at 0.62 g/MJ, 0.61 g/MJ, and 0.46 g/MJ for 5% FWB_A, 10% FWB_A, and 15% FWB_A, respectively. These results show that low ash deposition occurred when employing a 15% FWB_A cofiring ratio. Therefore, the combustion of FWB_A appears to be advantageous in terms of ash deposition mitigation.

3.4. TMA Characteristics

The fusion or melting behavior of biomass at elevated temperatures during combustion exerts a direct influence on combustion efficiency. During biomass combustion, inorganic components such as ash and volatile matter undergo thermal transformations. When the ash fusion temperature is low, the ash particles tend to melt, forming sticky deposits on the surface of the combustion reactor. This slag-like residue can disrupt airflow and hinder the overall combustion efficiency. Furthermore, local oxygen-deficient zones can be formed by these slaggy ash deposits, contributing to incomplete combustion of solid fuel and increased emissions of pollutants such as CO, SO₂, particulate matter, and volatile organic compounds [38,39]. Thus, understanding and controlling the ash fusion phenomenon hold paramount importance in reducing pollutant emissions and optimizing combustion conditions. To this end, we conducted an ash fusion experiment using TMA to assess the ash fusion tendencies of biomass fuels.

As shown in Figure 5, both coal and FWBs exhibit secondary to tertiary fusion points rather than a singular, distinctive fusion point. This indicates the heterogeneity and nonuniformity of ash derived from biomass combustion. Coal displayed a primary fusion range between 800 °C and 1100 °C, followed by a rapid secondary fusion between 1400 °C and 1500 °C, as evident in the TMA results (Figure 5). Specific temperature points T25, T50, T75, and T90 for coal were recorded at 1095 °C, 1454 °C, 1494 °C, and 1512 °C, respectively. Conversely, FWB_A exhibited a more intricate fusion behavior than that of general biomass, manifesting at three different fusion rates. Its primary fusion was between 800 °C and 900 °C, followed by a gradual secondary fusion between 1000 °C and 1400 °C, and a tertiary fusion between 1400 °C and 1500 °C. For FWB_A, the temperature values for T25, T50, T75, and T90 were measured at 926 °C, 1258 °C, 1458 °C, and 1504 °C, respectively, depicting fusion characteristics relatively akin to those of coal. FWB_B exhibited a solitary, distinct fusion point occurring between 1400 °C and 1500 °C. The corresponding temperature values for T25, T50, T75, and T90 were 1431 °C, 1484 °C, 1516 °C, and 1532 °C, respectively. In the case of FWB_B, the fusion of the entire ash component occurred at a relatively high temperature, and single fusion occurred at a temperature higher than that of coal. Both FWBs exhibited elevated fusibility levels akin to those of coal, suggesting compatibility in ash fusion temperatures for FWB and coal and implies that cofiring of these fuels can be more efficient and environmentally friendly. Sewage sludge has a lower fusion point than that of coal and FWB, consistent with the general characteristics of biomass fuels [40,41]. The fusion points of sewage sludge were determined to be 910 °C, 951 °C, 977 °C, and 993 °C, which all fall below 1000 °C. In a previous study, the high metal content in sewage sludge was identified as the main factor responsible for the low ash fusion temperature [40].

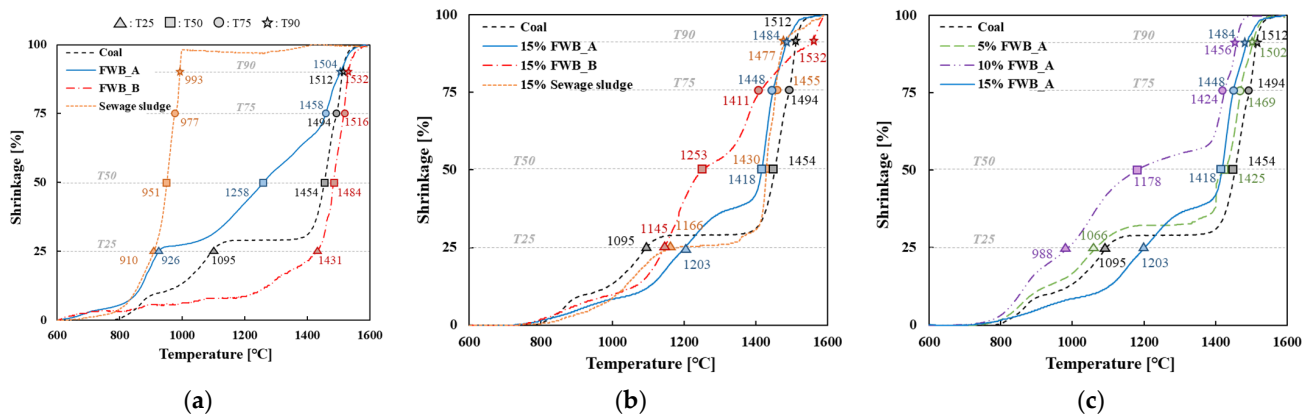


Figure 5. Thermomechanical analysis results of FWB_A (blue line), FWB_B (orange dot line), sewage sludge (yellow dot line), and coal (black dot line). (a) Shrinkage (%) of biomass fuels and coal as a function of temperature. (b) Shrinkage of co-combustion of biomass fuels and coal. (c) Shrinkage of co-combustion of FWB_A and coal with varying ratios.

The fusion tendency of the actual ash was not represented by the TMA results of the single ash components or the combined trends extracted from each TMA result. Furthermore, the fusion temperature of biomass ash depends on its chemical composition [42]. Solid fuels with heterogeneous ash components exhibit inconsistent fusion characteristics during co-combustion, rendering predictions of ash fusion points inherently challenging.

The fusion characteristics during co-combustion were examined by comparing the TMA results of 15% cofiring with each biomass (Figure 5b). The primary fusion of 15% FWB_A was observed between 800 °C and 1300 °C, followed by a distinctive secondary fusion between 1400 °C and 1500 °C (T25 at 1203 °C, T50 at 1418 °C, T75 at 1448 °C, and T90 at 1484 °C). Notably, FWB_A exhibited a higher first fusion temperature (T25) than that of 100% coal, albeit its T75 and T90 were lower than those of coal. A single gradual fusion was observed in 15% FWB_B. Notably, FWB_B showed the lowest fusibility up to T75 during a single combustion and the highest fusion temperature at T90 when cofired at 15% with coal. This trend was attributed to the inherently high fusion temperature of FWB_B during single combustion. A distinct single fusion was observed for 15% sewage sludge between 1400 °C and 1500 °C, similar to the tendency of coal, and in the case of 15% sewage sludge, T25 was at 1166 °C, T50 at 1430 °C, T75 at 1455 °C, and T90 at 1477 °C. Overall, coal played a dominant role in the fusion of FWB_A and sewage sludge, leading to an increase in fusibility.

Finally, a TMA fusion analysis was conducted on the co-combustions of 5% FWB_A, 10% FWB_A, and 15% FWB_A. The co-combustion of 5% FWB_A showed a similar tendency to that of coal but with a slightly lower fusion point. In the case of 5% FWB_A, primary fusion occurred between 800 °C and 1100 °C, followed by a rapid secondary fusion between 1400 °C and 1500 °C (T25 at 1066 °C, T50 at 1425 °C, T75 at 1469 °C, and T90 at 1502 °C). The co-combustion of 10% FWB_A had the lowest fusion point, and this is presumed to be due to the eutectic phenomenon. Primary fusion was observed between 800 °C and 1400 °C, and a drastic secondary fusion was observed between 1400 °C and 1500 °C. The fusion points were relatively low, which is unfavorable for co-combustion. High alkaline oxides such as CaO and MgO in biomass lower the ash melting tendencies, whereas SiO₂ and Al₂O₃ have a negative effect on the ash fluidity of the coal [43]. High CaO content in FWB, compared to coal, may decrease fusion temperature (Table 3). Fusibility did not decrease with an increase in the co-combustion ratio. Furthermore, the fusibility at blending rates of 5% and 15% did not differ significantly from that of the single combustion of coal. In summary, at single fusion, sewage sludge exhibited the lowest fusion point and poor melting properties, whereas relatively superior fusion characteristics were shown for FWB_A and FWB_B. Understanding the ash fusion characteristics of biomass contributes to the establishment of appropriate measures to prevent slagging issues and enhances the combustion efficiency of biomass. To minimize ash deposition and optimize combustion efficiency, the cofiring ratio or blending of solid fuel can be adjusted. These efforts may promote environmentally friendly biomass combustion.

Table 3. XRF analysis results of ash components of solid fuels.

	Coal	FWB_A	FWB_B	Sewage Sludge
SiO ₂	86.02	4.36	6.56	25.00
Al ₂ O ₃	9.25	0.00	0.00	16.53
Fe ₂ O ₃	2.23	0.97	1.63	12.21
CaO	0.00	61.18	53.17	9.38
MgO	0.00	2.81	4.04	0.85
Na ₂ O	0.00	0.00	0.00	0.00
K ₂ O	0.00	2.30	0.78	2.68
SO ₃	0.00	2.68	3.51	0.01
P ₂ O ₅	0.00	20.74	21.43	26.37
Etc.	2.50	5.0	8.9	7.0

3.5. Grindability Evaluation

The grindability of biomass, which is its ability to be pulverized into smaller particles, directly influences the efficiency and effectiveness of biomass combustion. Biomass needs to be ground to improve its combustion efficiency and heat transfer rates. In addition, solid fuels with high grindability have advantages in handling and storage because fuel transportation and storage are more convenient and experience fewer bridging or blockage problems.

The grindability of the biomass was evaluated based on the TTBTGI [29]. As shown in Figure 6, the TTBTGI values of FWB_A and FWB_B were higher than those of coal and sewage sludge. Coal with TTBTGI 36% was classified as very hard, sewage sludge with TTBTGI 43% was classified as hard, and FWB_A and FWB_B with TTBTGI values were 80% and 75% each, so they were classified as medium-hard. In general, solid biomass fuels have low grindability because of their high moisture content, irregular particle shape, and biomass size. The heterogeneous composition of the biomass, including its inorganic ash content, also results in low grindability. In particular, alkali metals in ash may cause wear and damage to grinding equipment. However, in this study, high grindability using FWB was achieved, likely due to the pyrolysis process. Such preprocessing reduces the moisture and inorganic ash contents of biomass fuel. The higher grindability of the solid fuel suggests that it is an efficient cofiring fuel that requires less power consumption during fuel preparation.

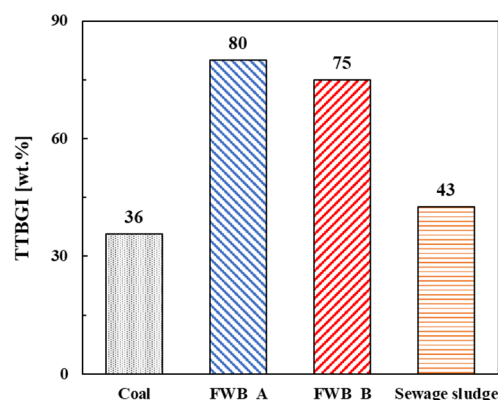


Figure 6. Grindability evaluation of biomass fuels and coal using the Thermally Treated Biomass Grindability Index.

4. Conclusions

FWB was prepared and evaluated as a cofiring biomass fuel in this study. Combustibility, ash deposition characteristics, ash fusion tendencies, and grindability of FWB during co-combustion were investigated. The following conclusions were drawn from this study:

- I. FWBs showed similar calorific values with coal, approximately 2000 kcal/kg higher than that of sewage sludge fuel.
- II. The gaseous emissions of NO_x and UBC from the combustion of FWB indicated environmental benefits, especially at a 10% mixing ratio.
- III. FWB_A exhibited melting behavior at low temperatures, indicating a potential negative impact on ash fouling and slagging. Similar fusion characteristics of FWB_A to coal make it a more suitable cofiring resource. Lower fusion points for sewage sludge imply potential operational issues.
- IV. FWBs demonstrated higher grindability compared to traditional biomass fuels due to the pyrolysis process. This high grindability is beneficial for fuel preparation, transportation, and storage, reducing overall operational costs.

The findings of this study suggest that FWB_A is a valuable resource for co-combustion in coal-fired power plants. Because the current study was limited to lab-scale experiments using DTF, the findings cannot be generalized to the actual application of FWB in coal-fired

power plants. Therefore, further studies are required to validate the feasibility of using FWB in coal-fired power plants. Continued efforts in both research and energy policy are required to make the FWB a more efficient renewable resource.

Author Contributions: Conceptualization, I.-T.K. and C.-H.J.; methodology, D.-C.S. and S.-M.K.; validation, Y.J., J.-S.K. and Y.-E.L.; formal analysis, K.-H.K. and M.-J.K.; investigation, K.-H.A. and J.J.; writing—original draft preparation, Y.J.; writing—review and editing, Y.J. and J.-S.K.; visualization, J.-S.K.; supervision, I.-T.K. and C.-H.J.; project administration, I.-T.K. All authors have read and agreed to the published version of the manuscript.

Funding: This research was funded by the Korea Institute of Civil Engineering and Building Technology (KICT) (grant number 20230094-001).

Informed Consent Statement: Not applicable.

Data Availability Statement: Not applicable.

Conflicts of Interest: The authors declare no conflict of interest.

References

- Goerndt, M.E.; Aguilar, F.X.; Skog, K. Drivers of Biomass Co-Firing in U.S. Coal-Fired Power Plants. *Biomass Bioenergy* **2013**, *58*, 158–167. [[CrossRef](#)]
- Savolainen, K. Co-Firing of Biomass in Coal-Fired Utility Boilers. *Appl. Energy* **2003**, *74*, 369–381. [[CrossRef](#)]
- Unchaisri, T.; Fukuda, S. Investigation of Ash Formation and Deposit Characteristics in CFB Co-Combustion of Coal with Various Biomass Fuels. *J. Energy Inst.* **2022**, *105*, 42–52. [[CrossRef](#)]
- García, R.; Pizarro, C.; Lavín, A.G.; Bueno, J.L. Characterization of Spanish Biomass Wastes for Energy Use. *Bioresour. Technol.* **2012**, *103*, 249–258. [[CrossRef](#)] [[PubMed](#)]
- Padeyanda, Y.; Jang, Y.-C.; Ko, Y.; Yi, S. Evaluation of Environmental Impacts of Food Waste Management by Material Flow Analysis (MFA) and Life Cycle Assessment (LCA). *J. Mater. Cycles Waste Manag.* **2016**, *18*, 493–508. [[CrossRef](#)]
- Lee, Y.-E.; Shin, D.-C.; Jeong, Y.; Kim, I.-T.; Yoo, Y.-S. Effects of Pyrolysis Temperature and Retention Time on Fuel Characteristics of Food Waste Feedstuff and Compost for Co-Firing in Coal Power Plants. *Energies* **2019**, *12*, 4538. [[CrossRef](#)]
- Pahla, G.; Ntuli, F.; Muzenda, E. Torrefaction of Landfill Food Waste for Possible Application in Biomass Co-Firing. *Waste Manag.* **2018**, *71*, 512–520. [[CrossRef](#)] [[PubMed](#)]
- Wei, X.; Lopez, C.; von Puttkamer, T.; Schnell, U.; Unterberger, S.; Hein, K.R.G. Assessment of Chlorine–Alkali–Mineral Interactions during Co-Combustion of Coal and Straw. *Energy Fuels* **2002**, *16*, 1095–1108. [[CrossRef](#)]
- Niu, Y.; Tan, H.; Hui, S. Ash-Related Issues during Biomass Combustion: Alkali-Induced Slagging, Silicate Melt-Induced Slagging (Ash Fusion), Agglomeration, Corrosion, Ash Utilization, and Related Countermeasures. *Prog. Energy Combust. Sci.* **2016**, *52*, 1–61. [[CrossRef](#)]
- Yao, X.; Zhao, Z.; Li, J.; Zhang, B.; Zhou, H.; Xu, K. Experimental Investigation of Physicochemical and Slagging Characteristics of Inorganic Constituents in Ash Residues from Gasification of Different Herbaceous Biomass. *Energy* **2020**, *198*, 117367. [[CrossRef](#)]
- Nutalapati, D.; Gupta, R.; Moghtaderi, B.; Wall, T.F. Assessing Slagging and Fouling during Biomass Combustion: A Thermodynamic Approach Allowing for Alkali/Ash Reactions. *Fuel Process. Technol.* **2007**, *88*, 1044–1052. [[CrossRef](#)]
- Ma, T.; Fan, C.; Hao, L.; Li, S.; Song, W.; Lin, W. Fusion Characterization of Biomass Ash. *Thermochim. Acta* **2016**, *638*, 1–9. [[CrossRef](#)]
- Tortosa Masiá, A.A.; Buhre, B.J.P.; Gupta, R.P.; Wall, T.F. Characterising Ash of Biomass and Waste. *Fuel Process. Technol.* **2007**, *88*, 1071–1081. [[CrossRef](#)]
- Cai, J.; He, Y.; Yu, X.; Banks, S.W.; Yang, Y.; Zhang, X.; Yu, Y.; Liu, R.; Bridgwater, A.V. Review of Physicochemical Properties and Analytical Characterization of Lignocellulosic Biomass. *Renew. Sustain. Energy Rev.* **2017**, *76*, 309–322. [[CrossRef](#)]
- Bridgeman, T.G.; Jones, J.M.; Shield, I.; Williams, P.T. Torrefaction of Reed Canary Grass, Wheat Straw and Willow to Enhance Solid Fuel Qualities and Combustion Properties. *Fuel* **2008**, *87*, 844–856. [[CrossRef](#)]
- Weber, R. Relevance of BFRs and Thermal Conditions on the Formation Pathways of Brominated and Brominated–Chlorinated Dibenzodioxins and Dibenzofurans. *Environ. Int.* **2003**, *29*, 699–710. [[CrossRef](#)] [[PubMed](#)]
- Lee, D.-G.; Ku, M.-J.; Kim, K.-H.; Kim, J.-S.; Kim, S.-M.; Jeon, C.-H. Experimental Investigation of the Ash Deposition Characteristics of Biomass Pretreated by Ash Removal during Co-Combustion with Sub-Bituminous Coal. *Energies* **2021**, *14*, 7391. [[CrossRef](#)]
- ASTM Standard D3173-11; Standard Test Method for Moisture in the Analysis Sample of Coal and Coke. ASTM International: West Conshohocken, PA, USA, 2011.
- ASTM Standard D3175-11; Standard Test Method for Volatile Matter in the Analysis Sample of Coal and Coke. ASTM International: West Conshohocken, PA, USA, 2011.
- ASTM D3174-12; Standard Test Method for Ash in the Analysis Sample of Coal and Coke from Coal. ASTM International: West Conshohocken, PA, USA, 2011.

21. ASTM D3172-13(2021)e1; Standard Practice for Proximate Analysis of Coal and Coke. ASTM International: West Conshohocken, PA, USA, 2021.
22. ASTM D5865; Standard Test Method for Gross Calorific Value of Coal and Coke. ASTM International: West Conshohocken, PA, USA, 2011.
23. DIN 51729-10; Testing of Solid Fuels-Determination of Chemical Composition of Fuel Ash-Part 10: X-ray Fluorescence Analysis. Deutsches Institut für Normung: Berlin, Germany, 2011.
24. Wu, Z.; Wang, S.; Zhao, J.; Chen, L.; Meng, H. Product distribution during co-pyrolysis of bituminous coal and lignocellulosic biomass major components in a drop-tube furnace. *Energy Fuels* **2015**, *29*, 4168–4180. [\[CrossRef\]](#)
25. Chen, W.-H.; Du, S.-W.; Tsai, C.-H.; Wang, Z.-Y. Torrefied Biomasses in a Drop Tube Furnace to Evaluate Their Utility in Blast Furnaces. *Bioresour. Technol.* **2012**, *111*, 433–438. [\[CrossRef\]](#)
26. Barroso, J.; Ballester, J.; Ferrer, L.M.; Jiménez, S. Study of Coal Ash Deposition in an Entrained Flow Reactor: Influence of Coal Type, Blend Composition and Operating Conditions. *Fuel Process. Technol.* **2006**, *87*, 737–752. [\[CrossRef\]](#)
27. Blanchard, R. Measurements and Modeling of Coal Ash Deposition in an Entrained-Flow Reactor. Master's Thesis, Brigham Young University, Provo, UT, USA, 2008.
28. JIS M8801; Coal-Testing Methods. Japanese Standards Association (JSA): Tokyo, Japan, 2008.
29. Yu, S.; Park, J.; Kim, M.; Kim, H.; Ryu, C.; Lee, Y.; Yang, W.; Jeong, Y.-G. Improving Energy Density and Grindability of Wood Pellets by Dry Torrefaction. *Energy Fuels* **2019**, *33*, 8632–8639. [\[CrossRef\]](#)
30. Huang, X.; Ng, K.W.; Giroux, L. Grindability of biocarbon and coal blends in rolling mill. *Int. J. Coal Prep. Util.* **2022**, *42*, 1651–1663. [\[CrossRef\]](#)
31. Ndibe, C.; Grathwohl, S.; Paneru, M.; Maier, J.; Scheffknecht, G. Emissions Reduction and Deposits Characteristics during Cofiring of High Shares of Torrefied Biomass in a 500 KW Pulverized Coal Furnace. *Fuel* **2015**, *156*, 177–189. [\[CrossRef\]](#)
32. Loeffler, D.; Anderson, N. Emissions Tradeoffs Associated with Cofiring Forest Biomass with Coal: A Case Study in Colorado, USA. *Appl. Energy* **2014**, *113*, 67–77. [\[CrossRef\]](#)
33. Kouprianov, V.I.; Permchart, W. Emissions from a Conical FBC Fired with a Biomass Fuel. *Appl. Energy* **2003**, *74*, 383–392. [\[CrossRef\]](#)
34. Permchart, W.; Kouprianov, V.I. Emission Performance and Combustion Efficiency of a Conical Fluidized-Bed Combustor Firing Various Biomass Fuels. *Bioresour. Technol.* **2004**, *92*, 83–91. [\[CrossRef\]](#) [\[PubMed\]](#)
35. Sun, P.; Hui, S.; Gao, Z.; Zhou, Q.; Tan, H.; Zhao, Q.; Xu, T. Experimental Investigation on the Combustion and Heat Transfer Characteristics of Wide Size Biomass Co-Firing in 0.2 MW Circulating Fluidized Bed. *Appl. Therm. Eng.* **2013**, *52*, 284–292. [\[CrossRef\]](#)
36. Demirbas, A. Potential Applications of Renewable Energy Sources, Biomass Combustion Problems in Boiler Power Systems and Combustion Related Environmental Issues. *Prog. Energy Combust. Sci.* **2005**, *31*, 171–192. [\[CrossRef\]](#)
37. Pronobis, M. The Influence of Biomass Co-Combustion on Boiler Fouling and Efficiency. *Fuel* **2006**, *85*, 474–480. [\[CrossRef\]](#)
38. Wang, L.; Tang, C.; Zhu, T.; Fang, F.; Ning, X.; Che, D. Experimental Investigation on Combustion and NO_x Formation Characteristics of Low-Ash-Melting-Point Coal in Cyclone Furnace. *ACS Omega* **2022**, *7*, 26537–26548. [\[CrossRef\]](#)
39. Kleinhans, U.; Wieland, C.; Frandsen, F.J.; Spliethoff, H. Ash Formation and Deposition in Coal and Biomass Fired Combustion Systems: Progress and Challenges in the Field of Ash Particle Sticking and Rebound Behavior. *Prog. Energy Combust. Sci.* **2018**, *68*, 65–168. [\[CrossRef\]](#)
40. Zhou, A.; Wang, X.; Magdziarz, A.; Yu, S.; Deng, S.; Bai, J.; Zhang, Q.; Tan, H. Ash Fusion and Mineral Evolution during the Co-Firing of Coal and Municipal Sewage Sludge in Power Plants. *Fuel* **2022**, *310*, 122416. [\[CrossRef\]](#)
41. Namkung, H.; Lee, Y.-J.; Park, J.-H.; Song, G.-S.; Choi, J.W.; Choi, Y.-C.; Park, S.-J.; Kim, J.-G. Blending Effect of Sewage Sludge and Woody Biomass into Coal on Combustion and Ash Agglomeration Behavior. *Fuel* **2018**, *225*, 266–276. [\[CrossRef\]](#)
42. Nunes, L.J.R.; Matias, J.C.O.; Catalão, J.P.S. Biomass Combustion Systems: A Review on the Physical and Chemical Properties of the Ashes. *Renew. Sustain. Energy Rev.* **2016**, *53*, 235–242. [\[CrossRef\]](#)
43. Wang, H.; Cheng, L.; Pu, J.; Zhao, J. Melting Characteristics of Coal Ash and Properties of Fly Ash to Understand the Slag Formation in the Shell Gasifier. *ACS Omega* **2021**, *6*, 16066–16075. [\[CrossRef\]](#)

Disclaimer/Publisher's Note: The statements, opinions and data contained in all publications are solely those of the individual author(s) and contributor(s) and not of MDPI and/or the editor(s). MDPI and/or the editor(s) disclaim responsibility for any injury to people or property resulting from any ideas, methods, instructions or products referred to in the content.